Gondwana Research xxx (2012) xxx–xxx

Contents lists available at SciVerse ScienceDirect

Gondwana Research

journal homepage: www.elsevier.com/locate/gr

Global warming and South Indian monsoon rainfall—lessons from the Mid-Miocene

Markus Reuter [a,*], Andrea K. Kern [b], Mathias Harzhauser [b], Andreas Kroh [b], Werner E. Piller [a]

[a] Institute for Earth Sciences, University of Graz, Heinrichstraße 26, 8010, Graz Austria
[b] Department of Geology and Palaeontology, Natural History Museum Vienna, Burgring 7, 1010 Vienna, Austria

ARTICLE INFO

Article history:
Received 4 April 2012
Received in revised form 5 July 2012
Accepted 19 July 2012
Available online xxxx

Handling Editor: P. Eriksson

Keywords:
Global warming
Indian monsoon
Coexistence Approach
Middle Miocene Climate Optimum
South India

ABSTRACT

Precipitation over India is driven by the Indian monsoon. Although changes in this atmospheric circulation are caused by the differential seasonal diabatic heating of Asia and the Indo-Pacific Ocean, it is so far unknown how global warming influences the monsoon rainfalls regionally. Herein, we present a Miocene pollen flora as the first direct proxy for monsoon over southern India during the Middle Miocene Climate Optimum. To identify climatic key parameters, such as mean annual temperature, warmest month temperature, coldest month temperature, mean annual precipitation, mean precipitation during the driest month, mean precipitation during the wettest month and mean precipitation during the warmest month the Coexistence Approach is applied. Irrespective of a ~3–4 °C higher global temperature during the Middle Miocene Climate Optimum, the results indicate a modern-like monsoonal precipitation pattern contrasting marine proxies which point to a strong decline of Indian monsoon in the Himalaya at this time. Therefore, the strength of monsoon rainfall in tropical India appears neither to be related to global warming nor to be linked with the atmospheric conditions over the Tibetan Plateau. For the future it implies that increased global warming does not necessarily entail changes in the South Indian monsoon rainfall.

1. Introduction

Asian monsoon is a substantial component of the global climate system, which affects half of the world's population (An, 2000; Lovett, 2010). This large-scale atmospheric circulation comprises the Indian and East Asian monsoon subsystems, both characterised by seasonal reversing winds and precipitation changes associated with asymmetric heating of land and sea. Temporal and spatial variability in these atmospheric circulations can result in severe droughts or floods with profound socioeconomic impact on large, densely populated regions (Webster et al., 1998; Cook et al., 2010). Accordingly, monsoon prediction models have a high priority in many Asian countries and global warming incites the question: will the Asian monsoon strengthen or weaken in the future (DelSole and Shukla, 2002; Ashfaq et al., 2009; Cook et al., 2010)?

Climate proxies from critical times of changing monsoon intensity are important for a better understanding of the driving forces (Overpeck and Cole, 2007). The development of the Asian monsoon system is considered to be related to the Himalayan uplift and dated to the beginning of the Neogene (Raymo and Ruddiman, 1992; Guo et al., 2002). In particular, growth of the Tibetan Plateau has been cited as being a trigger for an Asian monsoon intensification (Molnar et al., 1993). The Neogene monsoon history is mainly reconstructed from chemical and physical weathering rates recorded in widely continuous marine sequences of the Indus Fan, Bengal Fan and South China Sea which, depending on the source physiography and sediment, indicate drier or wetter climates (Clift et al., 2008; Wan et al., 2010). These climate proxies display long-term variations of the East Asian monsoon in the catchment area of the Perl and Yangtze rivers (South China) as well as of the Indian monsoon in the catchments of the Indus and Ganges–Brahmaputra river systems (Himalaya; Clift et al., 2008; Wan et al., 2010). The overall trend is one of gradually increasing monsoon strength from the beginning of the Neogene to 10 Ma (Late Miocene) with an unusually dry period at the Early/Middle Miocene transition (16.5–15 Ma; Clift et al., 2008).

The southwest Indian state of Kerala is popularly known as the "Gateway of summer monsoon" over India (Krishnakumar et al., 2009) and receives locally more than 75% of the rain by the Indian monsoon (Simon and Mohnakumar, 2004). Herein, we present an Early/Middle Miocene pollen flora from the siliciclastic Ambalapuzha Formation at the coastal cliffs of Varkala in SW Kerala, which represents the first terrestrial precipitation proxy from the time before 10 Ma for entire southern India. It corresponds to a global warming event at ~17–15 Ma (Middle Miocene Climate Optimum, MMCO; Zachos et al., 2001), when the global annual surface temperature was on average about ~3–4 °C higher than present and equivalent to the warming predicted for the next century by the mid-range scenarios of the IPCC Fourth Assessment Report (You et al., 2009;

* Corresponding author.
E-mail addresses: markus.reuter@uni-graz.at (M. Reuter), andrea.kern@nhm-wien.ac.at (A.K. Kern), mathias.harzhauser@nhm-wien.ac.at (M. Harzhauser), andreas.kroh@nhm-wien.ac.at (A. Kroh), werner.piller@uni-graz.at (W.E. Piller).

1342-937X/$ – see front matter
http://dx.doi.org/10.1016/j.gr.2012.07.015

You, 2010). Therefore and since the general conditions such as palaeogeography and paleobathymetry were not greatly different from today, this global warming episode represents a possible analogue of future climate change (You, 2010).

The state of current knowledge of the Asian monsoon systems during this crucial time interval of climate change is only inferred from marine sediments (Clift et al., 2008; Wan et al., 2010). However, these proxies neither provide direct information to the seasonal distribution of temperature and rainfalls nor to the monsoon over tropical India. In order to quantify the climate seasonality in SW-India during the MMCO the Coexistence Approach (Mosbrugger and Utescher, 1997) is applied to the Varkala pollen flora.

2. Geological setting and stratigraphy

The studied outcrop is located in the Kerala Basin (SW-India) at the coastal cliffs at Varkala (Fig. 1). It exposes a 21-m-thick siliciclastic succession of the Ambalapuzha Formation conformably overlying carbonates of the Quilon Formation (Vaidyanadhan and Ramakrishnan, 2008). Elevation and denudation of the Western Ghats were the source for the siliciclastics (Campanile et al., 2008). Palynofloras from these deposits document their deposition in marginal marine brackish lagoons as well as brackish and freshwater swamps (Ramanujan, 1987). Exceptional is the mixed siliciclastic–carbonatic Quilon Formation, which is interbedded between siliciclastics of the underlying Mayyanad Formation and the overlying Ambalapuzha Formation (Vaidyanadhan and Ramakrishnan, 2008; Fig. 2). It represents a marine ingression during the Burdigalian (Reuter et al., 2011). Calcareous nannoplankton from the Quilon Formation indicates nannoplankton zone NN3 (Reuter et al., 2011). The herein studied siliciclastics follow directly above the Quilon Formation with a conformable contact (Vaidyanadhan and Ramakrishnan, 2008) pointing to a late Burdigalian to early Langhian age (Fig. 2).

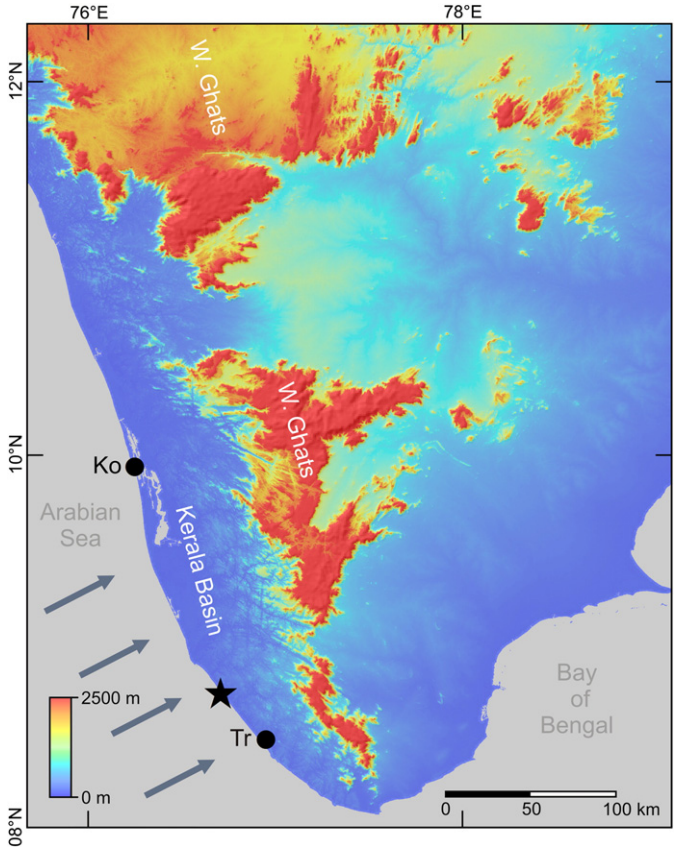

Fig. 1. Digital elevation model of southern India (Jarvis et al., 2008). The black asterisk locates the studied outcrop at Varkala (N 08°43′47″, E 076°42′30″) and the black dots indicate the position of the meterological stations Kochi (Ko) and Trivandrum (Tr). Blue arrows represent the SW-monsoon.

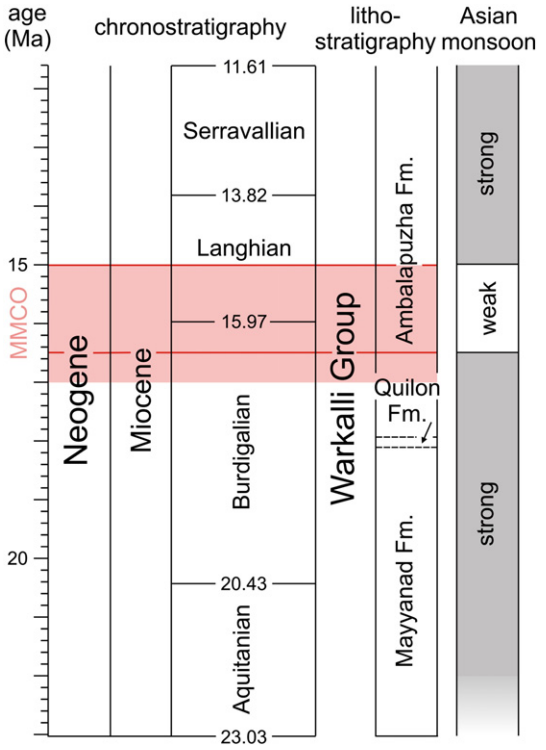

Fig. 2. Stratigraphic chart of the Varkala pollen flora. Correlation of the studied section with global chronostratigraphy (Gradstein et al., 2004), lithostratigraphy (Vaidyanadhan and Ramakrishnan, 2008), biostratigraphy (Reuter et al., 2011) and Asian monsoon intensity over northern India (Clift et al., 2008). The solid red lines mark the stratigraphic interval for the studied sediments, the red bar indicates the Middle Miocene Climate Optimum (MMCO).

In the studied section sediments range from bright yellow quartz sands to black sandy clays. Parts of the section exhibit lamination and flaser bedding due to interbedded laminae and lenses of well-sorted fine-grained quartz sands with finer grained dark grey muddy siliciclastics. In contrast, metre-thick yellow sand deposits show shallow inclined planar layers of well-sorted coarse-grained sand and fine gravel. Characteristically, the upper surfaces of these beds are erosive or modified by lateritic pedogenesis. Bioturbation is common in the sand as well as in the clay facies and predominantly represented by crab burrows. *Diplocraterion* ichnofossils can be associated in the clays as well as thin vertical rootlets of <20 cm length. Wood fragments occur in clay as well as sand facies.

3. Materials and methods

Eight samples were taken from dark grey and black sandy clays with a high amount of wood and/or rootlets. The samples were washed and processed with concentrated hydrochloric and hydrofluoric acid to eliminate silica and $CaCO_3$. Afterwards, the residues were preparated with concentrated glacial acetic acid before acetolysis was performed. At least 200 identified pollen grains were counted from each sample. Their identification stays at family and genus level to avoid parataxonomy.

The Coexistence Approach (CA; Mosbrugger and Utescher, 1997) was used for palaeoclimatic reconstructions. This method uses climatic tolerances of all nearest living relatives (NRLs) known for a fossil flora by assuming that the tolerances of a fossil taxon are not significantly different from its modern counterpart. The maximum overlap of the environmental tolerances of all the nearest living relatives is the coexistence interval (CI). By enquiring the Palaeoflora Database (Utescher

Please cite this article as: Reuter, M., et al., Global warming and South Indian monsoon rainfall—lessons from the Mid-Miocene, Gondwana Research (2012), http://dx.doi.org/10.1016/j.gr.2012.07.015

and Mosbrugger, 1997–2010), the palaeoclimatic parameters mean annual temperature (MAT), warmest month temperature (CMT), coldest month temperature (CMT), mean annual precipitation (MAT), mean precipitation during the driest month (MP_{dry}), mean precipitation during the wettest month (MP_{wet}) and mean precipitation during the warmest month (MP_{warm}) of the fossil pollen flora were calculated. For comparison with recent meteorological data (meteorological stations Kochi and Trivandrum) we consulted the WorldClimate database (http://www.worldclimate.com/; mean annual and monthly temperature, mean annual and monthly precipitation) and the Weather Information Service of the World Meteorological Organization (http://worldweather.wmo/; daily temperature range).

4. Results

In total, the Varkala pollen flora comprises 49 taxa belonging to 43 families—all still distributed in the tropical Indo-West Pacific region today (Table 1). Out of these 10 taxa of ecological importance have been treated at the genus level. Fine-grained siliciclastics with interlamination of sand and mud, lenticular, flaser and cross-bedding indicate deposits of the intertidal zone (Reineck, 1979). Sand-dominated fine-grained siliciclastic facies point to sand flat environments near the low-water line, while clay dominated facies is typical for higher intertidal mud flats that form near the high water line (Reineck, 1979). Bioturbation was mainly caused by crabs, which are typical inhabitants of mangroves, tidal flats and beaches. Associated *Diplocraterion* ichnofossils also indicate burrowing activity of intertidal *Corophium* amphipods (Yeo and Risk, 1981). In place tidal vegetation is documented by deep-reaching rootlets. Accordingly, pollen of mangrove vegetation (Rhizophoraceae, *Avicennia*, *Sonneratia*, *Nypa*, *Xylocarpus*; Thanikaimoni, 1987) are well represented in the studied pollen assemblages (Table 1).

Coarse-grained siliciclastic deposits with plane, gently dipping laminae of well-sorted coarse sand and fine gravel form in the swash zone (Reinson, 1984). Terrestrial episodes are documented by lateritic horizons. Stagnant or slowly flowing freshwater-influenced environments and evergreen lowland forests in the hinterland are indicated by *Myriophyllum*, Typhaceae, and Potamogetonaceae and Dipterocarpaceae pollen (Barboni et al., 2003; Table 1).

Since the qualitative composition of the pollen assemblages varies only slightly between the individual samples (Table 1), a low climate variability is indicated for the time interval covered by the studied sediment sequence. The CA analysis of the total Varkala pollen flora (Table 1) estimates a mean annual temperature of 24.4 °C (CI 22.2–26.6 °C) by a coldest month temperature of 21.7 °C (CI 20.6–22.8 °C) and a mean warmest month temperature of 28.1 °C. The mean annual precipitation is 1806 mm (CI 1748–1864 mm). On average 291.5 mm rainfall is calculated for the wettest month (CI 225–358 mm), 36.5 mm for the driest month (CI 18–55 mm) and 144.5 mm (CI 114–175 mm) for the warmest month (Table 2).

Table 1
Varkala pollen flora. Qualitative composition of the studied pollen assemblages and nearest living relatives of the recognised taxa.

Fossil pollen taxon	NRL	Sample							
		1	3	6	8	10	12	17	20
Acanthaceae	Acanthaceae	x	x	x	x	x		x	
Agavaceae	Agavaceae	x							
Anacardiaceae	Anacardiaceae	x	x	x	x	x	x	x	x
Apiaceae	Apiaceae	x		x			x	x	
Apocynaceae	Apocynaceae	x	x	x	x	x	x	x	x
Arecaceae	Arecaceae	x	x	x	x	x	x	x	x
Asteraceae	Asteraceae	x	x			x			
Avicennia	*Avicennia*	x	x	x	x	x	x	x	x
Bombacaceae	Bombacaceae	x		x	x	x		x	x
Brownlowia	Brownlowioideae		x				x	x	x
Caesalpiniaceae	*Caesalpina*	x	x	x	x	x	x	x	x
Calamus	*Calamus*	x	x	x	x	x	x	x	x
Chenopodiaceae	Chenopodiaceae		x		x		x		
Clusiaceae	Clusiaceae	x	x	x	x	x		x	x
Combretaceae	Combretaceae	x	x	x	x	x	x	x	x
Ctenolophaceae	Ctenolophaceae	x	x			x	x		x
Dipterocarpaceae	Dipterocarpaceae			x	x	x	x		
Droseraceae	Droseraceae					x		x	x
Euphorbiaceae	Euphorbiaceae	x	x	x	x	x	x	x	x
Fabaceae	Fabaceae	x	x	x		x		x	
Gunneraceae	Gunneraceae	x			x	x	x	x	x
Iridaceae	Iridaceae	x	x			x			
Lamiaceae	Lamiaceae	x	x	x		x	x	x	
Loranthaceae	Loranthaceae							x	
Malvaceae	Malvaceae	x	x	x	x	x	x	x	x
Menispermaceae	Menispermaceae		x	x				x	
Metroxylon	*Metroxylon*		x		x	x	x	x	
Moraceae	Moraceae	x	x	x	x	x	x	x	x
Myrriophyllum	*Myriophyllum*	x	x	x	x	x	x		x
Myrsinaceae	Myrsinaceae	x	x	x	x	x	x	x	x
Myrtaceae	Myrtaceae	x	x		x	x	x	x	x
Nypa	*Nypa*	x	x	x	x	x	x	x	x
Olacaceae	Olacaceae		x	x				x	
Oncosperma	*Oncosperma*	x	x	x	x	x	x	x	x
Plumbagiaceae	Plumbagiaceae	x	x	x	x	x	x	x	x
Poaceae	Poaceae		x	x	x	x	x		
Polygalaceae	Polygalaceae				x	x	x		x
Pontamogetaceae	Pontamogetaceae		x				x	x	x
Proteaceae	Proteaceae		x	x	x	x	x		x
Rhizophoraceae	Rhizophoraceae	x	x	x	x	x	x	x	x
Rubiaceae	Rubiaceae	x	x	x	x	x	x	x	x
Rutaceae	Rutaceae	x	x	x	x	x	x	x	x
Sapindaceae	Sapindaceae		x						
Sapotaceae	Sapotaceae	x	x	x	x	x	x	x	x
Symplocos	*Symplocos*	x						x	
Sonneratia	Sonneratiaceae	x	x	x	x	x	x	x	x
Tymeliaceae	Tymeliaceae	x	x	x		x	x	x	x
Typhaceae	Typhaceae	x			x			x	
Xylocarpus	*Xylocarpus*	x	x	x	x	x	x	x	x

5. Discussion

5.1. Climate characteristics of recent coastal Kerala

The principal rainy season in recent Kerala is between June and September during the SW-monsoon and in October–November during the NE-monsoon. During the winter months (December–February) occurs the lowest amount of rain (Simon and Mohnakumar, 2004). However, the rainfall intensity of coastal Kerala has a high spatial variability. It is profoundly influenced by the about 2500 m high mountain chain of the Western Ghats (Fig. 1), which catches the moisture from the Indian monsoon (Simon and Mohnakumar, 2004). Furthermore, the monsoon rainfall progresses from south to north along the west coast of India and

Table 2
Coexistence intervals and key taxa for the reconstructed palaeoclimatic parameters. Mean annual temperature (MAT), coldest month temperature (CMT), warmest month temperature (WMT), mean annual precipitation (MAP), mean precipitation during the wettest month (MP_{wet}), mean precipitation during the driest month (MP_{dry}) and mean precipitation during the warmest month (MP_{warm}).

Palaeoclimatic parameter		CI	Fossil pollen taxa
MAT (°C)	Minimum	22.2	Dipterocarpaceae, *Sonneratia*
	Maximum	26.6	*Calamus*
CMT (°C)	Minimum	20.6	*Brownlowia*
	Maximum	22.8	*Calamus*
WMT (°C)	Minimum	28.1	Dipterocarpaceae, Loranthaceae, Sapotaceae, *Sonneratia*
	Maximum	28.1	Anacardiaceae, Caesalpiniaceae
MAP (mm)	Minimum	1748	*Brownlowia*
	Maximum	1864	*Calamus*
MP_{wet} (mm)	Minimum	225	Dipterocarpaceae
	Maximum	358	Chenopodiaceae
MP_{dry} (mm)	Minimum	18	*Brownlowia*
	Maximum	55	*Calamus*
MP_{warm} (mm)	Minimum	114	*Brownlowia*
	Maximum	175	*Brownlowia*

Please cite this article as: Reuter, M., et al., Global warming and South Indian monsoon rainfall—lessons from the Mid-Miocene, Gondwana Research (2012), http://dx.doi.org/10.1016/j.gr.2012.07.015

creates differences in the rainfall characteristics between the southern and northern parts of recent Kerala. North Kerala (above 10°N) receives more than 75% of the annual rainfall during the SW-monsoon, south Kerala only 65–75% (Simon and Mohnakumar, 2004). June is the wettest month in south Kerala, while north Kerala experiences the highest rainfall in July (Simon and Mohnakumar, 2004). In addition, the southern tip receives only 25–30% of the annual rainfall during the pre-monsoon (March–May) and the NE-monsoon seasons. Precipitation during the pre-monsoon is mainly from thundershowers due to an increased thunderstorm activity in southernmost Kerala from March onwards (Simon and Mohnakumar, 2004). Most of the rainfall during the NE-monsoon is closely associated with the westward passage of storms and depressions, which are remnants of low pressure systems that move into the Bay of Bengal (Das, 1995). The tapering shape of the Indian peninsula and the lower elevation of the Western Ghats in the south (Fig. 1) are the main reasons for rainfall during this season in the southernmost part of Kerala (Simon and Mohnakumar, 2004).

The dry season is also the cold season (December–February) in SW coastal Kerala and characterised by a low daily minimum temperature. January is the coldest month. The warm season lasts from March to May (pre-monsoon) with April as warmest month (Simon and Mohnakumar, 2004).

5.2. Southwest Indian climate seasonality during the Middle Miocene Climate Optimum

Although located somewhat closer to the equator, the present shape of the Indian subcontinent existed already during Early/Middle Miocene (Scotese, 2002). Moreover, uplift of the Western Ghats and the creation of a steep escarpment facing the Arabian Sea started at ~50 Ma (Eocene) with a phase of major uplift during the Early Miocene (Gunell et al., 2003). Therefore, a modern-like regional topography may have already influenced the South Indian climate at the Early/Middle Miocene transition. For this reason it is necessary to use meteorological data from a similar geographic region (southwest coastal Kerala) for comparing Miocene and recent climate conditions. Because temperature and monthly precipitation data are not available from Varkala, the coastal meteorological stations Kochi and Trivandrum are chosen for comparison (Fig. 3a,b). Kochi is located 145 km north and Trivandrum 35 km south of Varkala (Fig. 1). The climate data from these meteorological stations display the very heterogeneous precipitation distribution at the recent Kerala coast with a decreasing rainfall seasonality towards the southern tip of India (Fig. 3a,b), while the mean annual temperature and the annual temperature cycle (Fig. 3a,b) of the stations are very similar.

The reconstructed climatic parameters for the Varkala pollen flora (Table 2) document a seasonal precipitation pattern with a dry and a wet period and moderate rainfalls during the warmest period. This seasonality is similar to that of the recent annual precipitation cycle in southern Kerala (Fig. 3a,b) and affirms the presence of a monsoon-like atmospheric circulation over South India during the Middle Miocene Climate Optimum (MMCO). The average value of the CI for the Miocene MAP is 40% lower than the MAP at Kochi and 16% lower than the MAP at Kerala, while the MAP at Trivandrum is not significantly different from the corresponding Miocene value (Fig. 4a). In contrast, the CIs for the Miocene MP_{wet}, MP_{dry} and MP_{warm} indicate a more balanced rainfall pattern with a wetter driest and warmest month but a drier wettest month compared to present (Fig. 3b). Because the rainfall seasonality weakens towards the south in coastal Kerala today (Fig. 3a,b), a decreased Miocene rainfall seasonality may have been a response to the more southernly palaeolatitude of India (Scotese, 2002). However, not the latitude but the distance to the southern tip of India is the critical constraint for the strength of seasonal rainfall in coastal Kerala (Simon and Mohnakumar, 2004). Taking the 16% lower Miocene MAP at Varkala into account (Fig. 4a) this points to a slightly more balanced

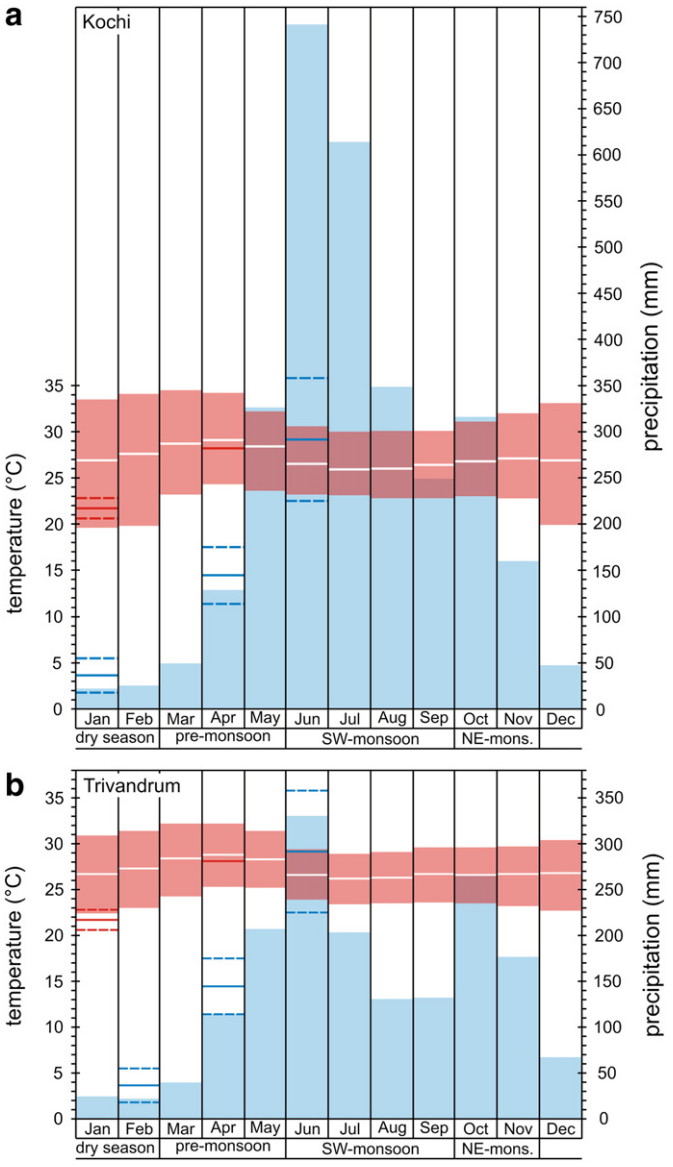

Fig. 3. Recent annual climate cycle in southern coastal Kerala. (a) Kochi. (b) Trivandrum. (a–b) The recent precipitation and temperature data are compiled after the Weather Information Service of the World Meteorological Organization (http://worldweather.wmo/; daily temperature range = red bars) and the WorldClimate database (http://www.worldclimate.com/; mean monthly temperature = solid white lines, mean monthly precipitation = blue columns). The dashed red (temperature) and blue (precipitation) lines show the coexistence intervals of the climatic parameter for the Varkala flora and the solid lines indicate the corresponding average values.

annual precipitation cycle in southern Kerala at the Early/Middle Miocene transition compared to today.

Despite of the close correlation of the Miocene and present annual rainfall cycles (Fig. 3) and a ~3–4 °C warmer global temperature during the MMCO (You et al., 2009), the mean value of the CI for the Miocene MAT lies significantly (~2.7 °C) below the recent MAT in coastal SW-Kerala (Fig. 4b). The estimated WMT is, however, in the same size order as today (Fig. 3a,b). Therefore, the low Miocene CMT (20.6–22.8 °C) has to account for the difference between the Miocene and the recent MAT pointing to a higher temperature seasonality and colder winter compared to today. However, this interpretation is problematic since as a basic principle tropical temperatures remain relatively constant throughout the year and the MMCO was characterised by higher equatorial sea surface temperatures and a weaker equator to pole latitudinal temperature gradient (Bruch et al., 2007; You et al., 2009). Notably, the CI for the Miocene CMT approximates the recent

Please cite this article as: Reuter, M., et al., Global warming and South Indian monsoon rainfall—lessons from the Mid-Miocene, Gondwana Research (2012), http://dx.doi.org/10.1016/j.gr.2012.07.015

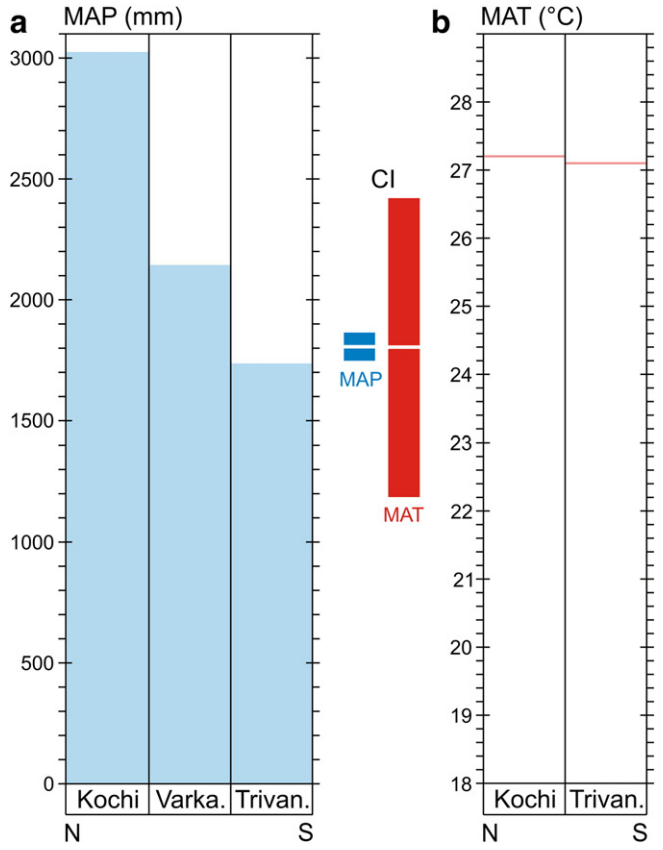

Fig. 4. North–south gradient of mean annual precipitation and mean annual temperature along the SW-coast of recent Kerala. (a) Mean annual precipitation (MAP). (b) Mean annual temperature (MAT). The recent climate data come from the WorldClimate database (http://www.worldclimate.com/). The blue and the red bar indicate the coexistence intervals (CI) for the Miocene MAP (blue) and MAT (red).

minimum 24-h temperature during the coldest month at Trivandrum and Kochi, which is significantly lower than the recent average CMT at these places (Fig. 3a,b). This suggests that the Miocene CMT displays only the lowest temperature during the year, which represents the lower temperature treshold for the tropical Varkala flora.

5.3. Influence of Miocene global warming and Himalaya uplift on South Indian monsoon

The CA for the Varkala flora indicates a modern-like tropical palaeoclimate. This result, however, contradicts weathering records from the Indus Fan and Bengal Fan (Clift et al., 2008), which indicate a breakdown of the Indian monsoon during the MMCO. The strength of the monsoon winds is regulated by a thermal gradient that develops from differential heating of land and sea (Webster et al., 1998). Of greatest relevance to the strength of the Indian monsoon is the temperature over the Tibetan Plateau region because it provides source for heating in the lower atmosphere during summer, that creates a vast low-pressure system over Central Asia, drawing in warm and humid air from the Indian Ocean towards the plateau (SW-monsoon; Goes et al., 2005). Although the timing of the uplift of the Tibetan Plateau is a matter of considerable debate (Wang et al., 2008), it has been shown that at least parts of the plateau reached their present altitude already during the MMCO (Spicer et al., 2003; Harris, 2006; Miao et al., 2012) and may have also influenced the Indian monsoon at this time. Nonetheless, the sediment records from the Arabian Sea and Bengal Bay, which are considered to display the palaeoclimate in the Himalaya region (Molnar et al., 1993), suggest a strong decline of the Indian monsoon during the MMCO implying a low thermal gradient between the Indian Ocean and the Tibetan Plateau. This is consistent with studies, which suggest increased warming at mid-latitudes (Flower and Kennett, 1994) and a weak equator to pole latitudinal temperature gradient during the MMCO (Bruch et al., 2007). In contrast, the Varkala pollen record, which mirrors the southern Indian palaeoclimate, does not reveal any significant differences between the MMCO and present-day climate seasonality. This result points to an increased N–S directed precipitation gradient over India compared to the recent and shows that the strength of monsoon rainfall in southern India was not significantly affected by warming of the Himalaya region during the Middle Miocene global warmth. In consistence with our findings the analysis of the interannual and decadal variability in summer monsoon rainfall over India and its teleconnections for the 1871–2001 period revealed that the Indian monsoon rainfall variability appears not to be linked with global warming and is decoupled from the Northern Hemisphere/Eurasian continent (Kripalani et al., 2003).

Despite of the strong similarities between the recent and Miocene annual climate cycles in southern Kerala, the CA for the Varkala flora documents also a slightly weaker Miocene rainfall seasonality (Figs. 3a,b and 4a). Compared to the strong Indian monsoon decline, which is inferred by the marine sediment records for the Himalaya region, this difference is only of little account. However, the present-day South Indian rainfalls are primarily related to the equatorial Indian Ocean and eastern Pacific sea surface temperatures (Chang et al., 2000) and the orography of southern India (Simon and Mohnakumar, 2004). Thus the more balanced distribution of the Mid-Miocene annual rainfall at Varkala seems to reflect rather a slight increase of the equatorial sea surface temperatures during the MMCO (You et al., 2009) than a decreased temperature gradient between the Indian Ocean and the Tibetan Plateau.

6. Conclusions

The pollen flora from the Early/Middle Miocene Ambalapuzha Formation at the southern Kerala coast presented here is the first direct proxy for Indian monsoon intensity over southern India during the MMCO. The CA was applied to this flora for the quantitative reconstruction of palaeoclimatic parameters (MAT, WMT, CMT, MAP, MP_{wet}, MP_{dry}, MP_{warm}). Irrespective of the warmer global climate during this period, the CA demonstrates a modern-like annual temperature and precipitation cycle with only slightly reduced rainfall seasonality. This strongly contrasts marine climate records that show a breakdown of the Indian monsoon over the Himalaya and South China. The decoupling of the Indian monsoon between North and South India during the MMCO shows that global warming had no significant effects on the Indian monsoon in low latitudes. In general, the temperature change during global warming is weak in low latitudes compared to mid-latitudes and accordingly the seasonal continent–ocean surface temperature gradient, which causes the Asian monsoon, is only slightly changing in equatorial regions.

Acknowledgements

We thank G. Jiménez-Moreno (Granada), who helped with pollen identification and literature, and T. Wagner (Graz) for the digital elevation model. A. Bruch (Frankfurt am Main) and T. Utescher (Bonn) are thanked for their constructive reviews. This research is a contribution to the NECLIME network and was funded by the FWF grants P18189, P21414 and P23492.

References

An, Z., 2000. The history and variability of the Asian paleomonsoon climate. Quaternary Science Reviews 19, 171–187.

Ashfaq, M., Shi, Y., Tung, W.-w., Trapp, R.J., Gao, X., Pal, J.S., Diffenbaugh, N.S., 2009. Suppression of south Asian summer monsoon precipitation in the 21st century. Geophysical Research Letters 36, L01704.

Barboni, D., Bonnefille, R., Prasad, S., Ramesh, B.R., 2003. Variation in the modern pollen from tropical evergreen forest and the monsoon seasonality gradient in SW India. Journal of Vegetation Science 14, 551–562.
Bruch, A.A., Uhl, D., Mosbrugger, V., 2007. Miocene climate in Europe. Patterns and evolution: A first synthesis of NECLIME. Palaeogeography, Palaeoclimatology, Palaeoecology 253, 1–7.
Campanile, D., Nambiar, C.G., Bishop, P., Widdowson, M., Brown, R., 2008. Sedimentation record in the Konkan-Kerala Basin: implications for the evolution of the Western Ghats and the Western Indian passive margin. Basin Research 20, 3–22.
Chang, C.-P., Zhang, Y., Li, T., 2000. Interannual and interdecadal variations of the East Asian summer monsoon and tropical Pacific SSTs. Part I: roles of the subtropical ridge. Journal of Climate 13, 4310–4325.
Clift, P.D., Hodges, K.V., Heslop, D., Hannigan, R., van Long, H., Calves, G., 2008. Correlation of Himalayan exhumation rates and Asian monsoon intensity. Nature Geoscience 1, 875–880.
Cook, E.R., Anchukaitis, K.J., Buckley, B.M., D'Arrigo, R.D., Jacoby, G.C., Wright, W.E., 2010. Asian monsoon failure and megadrought during the last millennium. Science 328, 486–489.
Das, P.K., 1995. The Monsoons. National Book Trust, New Delhi.
DelSole, T., Shukla, J., 2002. Linear prediction of Indian monsoon rainfall. Journal of Climate 15, 3645–3658.
Flower, B.P., Kennett, J.P., 1994. The Middle Miocene climate transition: East Antarctic ice sheet development, deep ocean circulation and global carbon cycling. Palaeogeography, Palaeoclimatology, Palaeoecology 108, 537–555.
Goes, J.I., Thoppil, P.G., Gomes, H., Fasullo, J.T., 2005. Warming of the Eurasian landmass is making the Arabian Sea more productive. Science 308, 545–547.
Gradstein, F.M., Ogg, J.G., Smith, A.G., 2004. A Geologic Time Scale 2004. Cambridge University Press, Cambridge.
Gunell, Y., Gallagher, K., Carter, A., Widdowson, M., Hurford, A.J., 2003. Denudation history of the continental margin of western peninsular India since the early Mesozoic—reconciling apatite fission-track data with geomorphology. Earth and Planetary Science Letters 215, 187–201.
Guo, Z., Ruddiman, W.F., Hao, Q.Z., Wu, H.B., Qian, Y.S., Zhu, R.X., Peng, S.Z., Wei, J.J., Yuan, B.Y., Liu, T.S., 2002. Onset of Asian desertification by 22 Ma ago inferred from loess deposits in China. Nature 416, 159–163.
Harris, N., 2006. The elevation history of the Tibetean Plateau and its implications for the Asian monsoon. Palaeogeography, Palaeoclimatology, Palaeoecology 241, 4–15.
Jarvis, A., Reuter, H.I., Nelson, E., Guevara, E., 2008. Hole-filled SRMT for the globe Version 4. CGIAR-CSI SRTM 90m Database. http://srtm.csi.cgiar.org.
Kripalani, R.H., Kulkarni, A., Sabade, S.S., Khandekar, M.L., 2003. Indian monsoon variability in a global warming scenario. Natural Hazards 29, 189–206.
Krishnakumar, K.N., Prasada Rao, G.S.L.H.V., Gopakumar, C.S., 2009. Rainfall trends in twentieth century over Kerala, India. Atmospheric Environment 43, 1940–1944.
Lovett, R.A., 2010. Tree rings map 700 years of Asian monsoons. Historical rainfall across the region documented for the first time. Nature News. http://dx.doi.org/10.1038/news.2010.196.
Miao, Y., Herrmann, M., Wu, F., Yan, X., Yang, S., 2012. What controlled Mid-Late Miocene long-term aridification in Central Asia? — Global cooling or Tibetan Plateau uplift: a review. Earth-Science Reviews 112, 155–172.
Molnar, P., England, P., Martinod, J., 1993. Mantle dynamics, uplift of the Tibetan Plateau, and the Indian Monsoon. Reviews of Geophysics 31, 357–396.
Mosbrugger, V., Utescher, T., 1997. The coexistence approach—a method for quantitative reconstructions of Tertiary terrestrial palaeoclimate data using plant fossils. Palaeogeography, Palaeoclimatology, Palaeoecology 134, 61–86.
Overpeck, T., Cole, J.E., 2007. Lessons from a distant monsoon. Nature 445, 270–271.
Ramanujan, C.G.K., 1987. Palynology of the Neogene Warkalli Beds of Kerala State in South India. Journal of the Palaeontological Society of India 32, 26–46.
Raymo, M.E., Ruddiman, W.F., 1992. Tectonic forcing of late Cenozoic climate. Nature 359, 117–122.
Reineck, H.-E., 1979. German North Sea tidal flats. In: Ginsburg, R.N. (Ed.), Tidal Deposits, A Casebook of Recent Examples and Fossil Counterparts. Springer-Verlag, Berlin Heidelberg New York, pp. 5–12.
Reinson, G.E., 1984. Barrier island and associated strand-plain systems. In: Walker, R.G. (Ed.), Facies models: Geoscience Canada Reprint Series, 1, pp. 119–140.
Reuter, M., Piller, W.E., Harzhauser, M., Kroh, A., Rögl, F., Coric, S., 2011. The Quilon Limestone, Kerala Basin, India: an archive for Miocene Indo-Pacific seagrass beds. Lethaia 44, 76–86.
Scotese, C.R., 2002. PALEOMAP website. http://www.scotese.com.
Simon, A., Mohnakumar, K., 2004. Spatial variability and rainfall characteristics of Kerala. Proceedings of the Indian Academy of Sciences: Earth and Planetary Sciences 113, 211–221.
Spicer, R.A., Harris, N.B.W., Widdowson, M., Herman, A.B., Guo, S., Valdes, P.J., Wolfe, J.A., Kelley, S.P., 2003. Constant elevation of southern Tibet over the past 15 million years. Nature 421, 622–624.
Thanikaimoni, G., 1987. Mangrove Palynology. UNDP/UNESCO Regional Project on Training and Research on Mangrove Ecosystems, RAS/79/002 and the French Institute, Pondicherry.
Utescher, T., Mosbrugger, V., 1997–2010. Palaeoflora Database. http://www.palaeoflora.de.
Vaidyanadhan, R., Ramakrishnan, M., 2008. Geology of India. Geological Society of India, Bangalore.
Wan, S., Clift, P.D., Li, A., Li, T., Yin, X., 2010. Geochemical records in the South China Sea: implications for East Asian summer monsoon evolution over the last 20 Ma. Monsoon Evolution and Tectonics—Climate linkage in Asia: In: Clift, P.D., Tada, R., Zheng, H. (Eds.), Geological Society, London, Special Publications, 342, pp. 245–263.
Wang, Y., Wang, X., Xu, Y., Zhang, C., Li, Q., Tseng, Z.J., Takeuchi, G., Deng, T., 2008. Stable isotopes in fossil mammals, fish and shells from Kunlun Pass Basin, Tibetan Plateau: Paleo-climatic and paleo-elevation implications. Earth and Planetary Science Letters 270, 73–85.
Webster, P.J., Magana, V.O., Palmer, T.N., Shukla, J., Tomas, R.A., Yanai, M., Yasunari, T., 1998. Monsoons: processes, predictability, and the prospects for prediction, in the TOGA decade. Journal of Geophysical Research 103, 14451–14510.
Yeo, R.K., Risk, M.J., 1981. The sedimentology, stratigraphy, and preservation of intertidal deposits in the Minas Basin System, Bay of Fundy. Journal of Sedimentary Petrology 51, 245–260.
You, Y., 2010. Climate-model evaluation of the contribution of sea-surface temperature and carbon dioxide to the Middle Miocene Climate Optimum as a possible analogue of future climate change. Australian Journal of Earth Sciences 57, 207–219.
You, Y., Huber, M., Müller, R.D., Poulsen, C.J., Ribbe, J., 2009. Simulation of the middle Miocene climate optimum. Geophysical Research Letters 36, L04702.
Zachos, J., Pagani, M., Sloan, L., Thomas, E., Billups, K., 2001. Trends, rhythms, and aberrations in global climate 65 Ma to present. Science 292, 686–693.

Please cite this article as: Reuter, M., et al., Global warming and South Indian monsoon rainfall—lessons from the Mid-Miocene, Gondwana Research (2012), http://dx.doi.org/10.1016/j.gr.2012.07.015